ISSN 0021-3640, JETP Letters, 2021, Vol. 114, No. 5, pp. 289–295. © Pleiades Publishing, Inc., 2021.
Russian Text © The Author(s), 2021, published in Pis'ma v Zhurnal Eksperimental'noi i Teoreticheskoi Fiziki, 2021, Vol. 114, No. 5, pp. 339–345.

CONDENSED MATTER

Implementation of the Concept of Spin Polaron in Cuprate Superconductors within the Diagram Technique

V. A. Mitskan[a], M. M. Korovushkin[a], and D. M. Dzebisashvili[a, *]

[a] *Kirensky Institute of Physics, Federal Research Center KSC, Siberian Branch, Russian Academy of Sciences, Krasnoyarsk, 660036 Russia*

**e-mail: ddm@iph.krasn.ru*

Received August 4, 2021; revised August 9, 2021; accepted August 9, 2021

The spectral properties of an ensemble of spin-polaron quasiparticles have been studied within the spin–fermion model of cuprate superconductors using the method combining the Feynman diagram technique and the diagram technique for spin operators. It has been shown that strong spin–charge coupling results in the formation of the lower spin-polaron band separated by a wide energy gap from the band of bare holes. It has been shown that the spin-polaron band has a local minimum near the $(\pi/2, \pi/2)$ point of the Brillouin zone. A class of diagrams for the self-energy part that have a fundamental significance for the description of the main features of the spin-polaron spectrum has been determined.

DOI: 10.1134/S0021364021170094

1. INTRODUCTION

The concept of spin polaron [1–4] is based on the strong spin–charge coupling [5–9], which exists in cuprate superconductors owing to strong electron correlations [10–13] and strong hybridization between d states of copper ions and p states of oxygen ions. Within this concept, the spin–charge coupling is taken into account exactly and this leads to the appearance of a fermion quasiparticle called spin polaron, whose motion strongly correlates with the dynamics of spins localized on the nearest copper ions.

The concept of spin polaron was developed within the Kondo lattice model [1–3, 14–16] and the spin–fermion model [17–22], which is an effective low-energy variant of the three-band Emery model [23, 24]. In particular, the spin–fermion model with real energy parameters made it possible to describe fine features of the electronic structure and spectral characteristics of spin-polaron quasiparticles [18, 19]. The main tool used in the cited studies is the Zwanzig–Mori projection technique [25–27], which in combination with the formalism of two-time retarded Green's functions allows the calculation of thermodynamic averages necessary for the description of both normal and superconducting properties of the ensemble of spin-polaron quasiparticles [20, 22, 28]. The specificity of this technique within the spin-polaron approach is the derivation of a closed system of equations for Green's functions on an extended set of basis operators, which correctly describe the strong spin–fermion coupling of quasiparticles on the CuO_2 plane. The main disadvantage of this approach is its mean-field character, which excludes the appropriate inclusion of the dynamic processes of spin–fluctuation scattering, which play an important role, e.g., in the description of the pseudogap phase of cuprate superconductors.

An attempt to develop the spin-polaron approach with the diagram technique referred to as the "bundle" technique was recently made in [29]. The specificity of this approach is the exact inclusion of the algebra of spin operators on one site, which makes it possible to correctly describe one-site processes of spin–charge scattering. However, the dependence of spin operators on the imaginary time is neglected in this approach, which prevents going beyond the static approximation.

The implementation of the concept of spin polaron proposed in this work is based on the combination of the well-developed diagram techniques for the fermion [30] and spin [31, 32] operators and is thereby free of disadvantages of previous approaches.

2. SPIN–FERMION MODEL

The Hamiltonian of the spin–fermion model [17, 33–37], which includes the main features of the electronic structure of the CuO_2 plane of high-temperature superconductors, has the form

$$\hat{H} = \sum_{k\alpha}(\xi_{k_x} a^{\dagger}_{k\alpha} a_{k\alpha} + \xi_{k_y} b^{\dagger}_{k\alpha} b_{k\alpha} + t_k (a^{\dagger}_{k\alpha} b_{k\alpha} + b^{\dagger}_{k\alpha} a_{k\alpha})) \quad (1)$$

$$+\frac{J}{N}\sum_{fkq\alpha\beta}e^{if(q-k)}u^{\dagger}_{k\alpha}\tilde{\mathbf{S}}^{\alpha\beta}_{f}u_{q\beta}+\frac{I}{2}\sum_{f\delta}\mathbf{S}_{f}\mathbf{S}_{f+2\delta}.$$

Here,

$$\xi_{k_{x(y)}}=\varepsilon_{p}-\mu+\tilde{\tau}\left(1-\cos k_{x(y)}\right),$$
$$t_{k}=\left(2\tilde{\tau}-4t\right)s_{k_{x}}s_{k_{y}},\quad s_{k_{x(y)}}=\sin(k_{x(y)}/2),$$
$$u_{k\beta}=s_{k_{x}}a_{k\beta}+s_{k_{y}}b_{k\beta},\quad \tilde{\mathbf{S}}_{f}=\mathbf{S}_{f}\sigma, \tag{2}$$
$$\tilde{\tau}=\frac{t^{2}_{pd}}{\Delta_{pd}}\left(1-\frac{\Delta_{pd}}{U_{d}-\Delta_{pd}}\right),$$
$$J=\frac{4t^{2}_{pd}}{\Delta_{pd}}\left(1+\frac{\Delta_{pd}}{U_{d}-\Delta_{pd}}\right).$$

The terms in the first sum in Eq. (1) describe the subsystem of holes on oxygen ions in the quasimomentum representation, where $a^{\dagger}_{k\alpha}(a_{k\alpha})$ and $b^{\dagger}_{k\alpha}(b_{k\alpha})$ are the operators of creation (annihilation) of a hole in the state with the quasimomentum k and spin projection $\alpha=\pm1/2$ in the subsystem of oxygen ions with the p_x and p_y orbitals, respectively. According to their definitions above, the functions $\xi_{k_{x(y)}}$ and t_k are expressed in terms of the binding energy of the hole on the oxygen ion ε_p, chemical potential μ, the direct hopping integral between the nearest oxygen ions t, and the parameter $\tilde{\tau}$ characterizing the intensity of hoppings of holes on oxygen owing to the second-order processes in the hybridization parameter t_{pd}. In the expression for $\tilde{\tau}$, $\Delta_{pd}=\varepsilon_p-\varepsilon_d$ is the gap with charge transfer, where ε_d is the one-site energy of the hole on the copper ion. The second sum in the Hamiltonian (1) describes the exchange interaction with the strength J between the subsystem of holes on oxygen and spins localized on copper ions. In this sum, $\tilde{\mathbf{S}}_f$ is the scalar product of the spin operator $\mathbf{S}_f$ on the fth site and the vector $\boldsymbol{\sigma}=(\sigma_x,\sigma_y,\sigma_z)$ whose components are the Pauli matrices, and N is the number of unit cells equal to the number of copper ions. The last sum in the Hamiltonian (1) describes the superexchange interaction with the strength I between the nearest spins on copper ions appearing in the fourth order of perturbation theory. In this sum, δ is the vector connecting a copper ion with the four nearest oxygen ions.

For the further consideration, it is convenient to represent the Hamiltonian of the spin–fermion model given by Eq. (1) in the representation of new fermion operators $\varphi_{k\alpha}$ and $\psi_{k\alpha}$, which can be defined through the following unitary transformation [38, 39]:

$$\varphi_{k\alpha}=\left(s_{k_{x}}a_{k\alpha}+s_{k_{y}}b_{k\alpha}\right)/\nu_{k},$$
$$\psi_{k\alpha}=\left(s_{k_{x}}b_{k\alpha}-s_{k_{y}}a_{k\alpha}\right)/\nu_{k}, \tag{3}$$

where $\nu_k=\sqrt{s^2_{k_x}+s^2_{k_y}}$. As a result, the Hamiltonian of the spin–fermion model is represented in the form

$$\hat{H}_{\text{s–f}}=\hat{H}_{0}+\hat{H}_{\text{int}} \tag{4}$$

convenient for the diagram technique. Here,

$$\hat{H}_{0}=\sum_{k\alpha}\left(\xi_{\psi k}\psi^{\dagger}_{k\alpha}\psi_{k\alpha}+\xi_{\varphi k}\varphi^{\dagger}_{k\alpha}\varphi_{k\alpha}\right)-\sum_{f}hS^{z}_{f} \tag{5}$$

is the operator that describes noninteracting oxygen holes and spins localized on copper ions, where

$$\xi_{\varphi k}=\varepsilon_{p}+2\tilde{\tau}\nu^{2}_{k}-8t\frac{s^{2}_{k_x}s^{2}_{k_y}}{\nu^{2}_{k}}-\mu,$$
$$\xi_{\psi k}=\varepsilon_{p}+8t\frac{s^{2}_{k_x}s^{2}_{k_y}}{\nu^{2}_{k}}-\mu. \tag{6}$$

The last term in Eq. (5) describes the Zeeman energy of spins in an infinitesimal field ($h\to0$) directed along the z axis and is added for the correct construction of the diagram technique for spin operators. In Eq. (4),

$$\hat{H}_{\text{int}}=\sum_{k\alpha}V_{k}(\varphi^{\dagger}_{k\alpha}\psi_{k\alpha}+\psi^{\dagger}_{k\alpha}\varphi_{k\alpha})$$
$$+\frac{1}{N}\sum_{kqf\alpha\beta}J_{kq}e^{if(q-k)}\varphi^{\dagger}_{k\alpha}\tilde{\mathbf{S}}^{\alpha\beta}_{f}\varphi_{q\beta}+\frac{I}{2}\sum_{f\delta}\mathbf{S}_{f}\mathbf{S}_{f+2\delta} \tag{7}$$

is the interaction operator, where

$$V_{k}=-4t\frac{s_{k_x}s_{k_y}}{\nu^{2}_{k}}(s^{2}_{k_x}-s^{2}_{k_y}),\quad J_{kq}=J\nu_{k}\nu_{q}.$$

The representation of the Hamiltonian in the form of Eq. (4) is convenient because only one type of bare quasiparticles (described by the operators $\varphi_{k\alpha}$) is coupled to the localized spin subsystem.

Below, we use an important feature of the interaction function J_{kq} related to the split character of this function.

3. GREEN'S FUNCTION OF HOLES AND THE SELF-ENERGY PART

To study the spectral properties of the system described by the Hamiltonian (4), we use the formalism of Matsubara Green's functions, which can be defined as

$$G^{(\varphi)}_{\alpha}(k,\tau-\tau')=-\left\langle T_{\tau}\tilde{\varphi}_{k\alpha}(\tau)\tilde{\varphi}^{\dagger}_{k\alpha}(\tau')\right\rangle,$$
$$G^{(\psi)}_{\alpha}(k,\tau-\tau')=-\left\langle T_{\tau}\tilde{\psi}_{k\alpha}(\tau)\tilde{\psi}^{\dagger}_{k\alpha}(\tau')\right\rangle. \tag{8}$$

Here, T_τ is the ordering operator in the Matsubara time variables τ and τ' varying from 0 to $\beta=1/T$, where T is the temperature, and

$$\tilde{\varphi}_{k\alpha}(\tau)=\exp(\tau\hat{H}_{\text{s–f}})\varphi_{k\alpha}\exp(-\tau\hat{H}_{\text{s–f}}) \tag{9}$$

is the operator φ in the Heisenberg representation; the expression for the operator ψ in the Heisenberg representation is similar. The angle brackets in Eq. (8) mean thermodynamic averaging with the density matrix determined by the Hamiltonian $\hat{H}_{s-f}$. It is important that the localized spin subsystem is in the quantum spin liquid state; i.e., the long-range magnetic order is absent ($\langle S_f^z \rangle = 0$) and the spin correlation functions $C_{fm} = 3\langle S_f^x S_m^x \rangle = 3\langle S_f^y S_m^y \rangle = 3\langle S_f^z S_m^z \rangle$ are SU(2)-invariant.

The Fourier transforms of Green's functions (8) have the form

$$G_\alpha^{(\eta)}(k,\tau) = T\sum_{\omega_m} e^{-i\omega_m\tau} G_\alpha^{(\eta)}(k, i\omega_n), \tag{10}$$

where $\omega_n = (2n+1)\pi T$, $n = 0, \pm1, \pm2, \ldots$ are the Matsubara frequencies and $\eta = \varphi, \psi$. The function $G_\alpha^{(\varphi)}(k, i\omega_n)$ satisfies the Dyson equation

$$G_\alpha^{(\varphi)}(k, i\omega_n) = \frac{1}{(G_k^{(0)}(i\omega_n))^{-1} - \Sigma(k, i\omega_n)}. \tag{11}$$

Here, $\Sigma(k, i\omega_n)$ is the irreducible part of the self-energy part and the function

$$G_k^{(0)}(i\omega_m) = \frac{i\omega_m - \xi_{\psi k}}{(i\omega_m - \xi_{\varphi k})(i\omega_m - \xi_{\psi k}) - V_k^2} \tag{12}$$

describes quasiparticles of type φ, which do not interact with the spin subsystem, taking into account their hybridization with quasiparticles of type ψ.

Further, we are interested in the regime of a low density of charge carriers, which is the case in cuprate superconductors. In this context, we indicate two important differences of the Hamiltonian of the spin–fermion model given by Eq. (4) from a formally similar Hamiltonian of the "extended" Kondo lattice model [4]. The first difference is the inequality $J \gg W$, where W is the hole bandwidh. It is a large value of J that responsible for the formation of spin-polaron quasiparticles in cuprates. In the Kondo lattice model, the opposite limit $J \ll W$ is usually considered. The second difference is a low hole density in cuprates $x < 0.2$. On the contrary, when describing the Kondo effect, it is important that the number of charge carriers is large because it ensures the efficient screening.

The low-density approximation in the diagram description makes it possible to omit all the diagrams containing fermion loops. It can be shown that the expression for the self-energy part describing the coupling of holes to the localized spin subsystem can be written in the form

$$\begin{aligned}\Sigma(k, i\omega_m) = J_{kk}\sum_{n=1}^{\infty}\frac{1}{N}\sum_{f_1\ldots f_n} T^n \int_0^\beta d\tau_1 \ldots d\tau_n \\ \times \sum_{\omega_1\ldots\omega_{n-1}} e^{i\tau_1(\omega_m-\omega_1)}\ldots e^{i\tau_n(\omega_{n-1}-\omega_m)} \\ \times X_{f_1-f_2}(i\omega_1)\ldots X_{f_{n-1}-f_n}(i\omega_{n-1}) \\ \times \left\langle T_\tau\left(\tilde{\mathbf{S}}_{f_1}(\tau_1)\ldots\tilde{\mathbf{S}}_{f_n}(\tau_n)\right)_{\downarrow\downarrow} \mathfrak{S}_I(\beta)\right\rangle_{0c}^{irr}.\end{aligned} \tag{13}$$

Here,

$$X_f(i\omega_l) = \frac{1}{N}\sum_q J_{qq} e^{iqf} G_k^{(0)}(i\omega_l), \tag{14}$$

$$\mathfrak{S}_I(\beta) = T_\tau \exp\left\{-\int_0^\beta d\tau \frac{I}{2}\sum_{f\delta}\mathbf{S}_f(\tau)\mathbf{S}_{f+2\delta}(\tau)\right\} \tag{15}$$

is the scattering matrix including interactions only between localized spins;

$$\tilde{\mathbf{S}}_f(\tau) = e^{\tau\tilde{H}_0}\tilde{\mathbf{S}}_f e^{-\tau\tilde{H}_0}, \quad \mathbf{S}_f(\tau) = e^{\tau\tilde{H}_0}\mathbf{S}_f e^{-\tau\tilde{H}_0} \tag{16}$$

are the matrix and vector spin operators in the interaction representation, respectively; the subscript 0 by the right angle bracket indicates that the thermodynamic average is taken with the density matrix describing the system without interaction; the next subscript c means that only coupled diagrams are taken into account to calculate the average of the product of spin operators according to the Wick theorem [31]; and the superscript irr indicates that only irreducible diagrams, i.e., diagrams that cannot be cut into two uncoupled parts over one fermion line, are taken into account. In view of the SU(2) invariance of the state of the spin subsystem, any diagonal element can be taken in the product of n matrix operators $\tilde{\mathbf{S}}_f(\tau)$. For definiteness, we take the $\downarrow\downarrow$ element.

4. SPIN GREEN'S FUNCTIONS

The T_τ-ordered thermodynamic average of each product of spin operators in Eq. (13) is calculated according to the general rules of the spin diagram technique [31]. A method for the calculation of the spin Green's functions in the one-loop approximation for systems in the quantum spin liquid state that are described within the spin–fermion model was developed in [40]. In particular, for the spin Green's function

$$\begin{aligned}D_{++}(f\tau; f'\tau') = -\langle T_\tau S_f^+(\tau) S_{f'}^-(\tau')\rangle \\ = \frac{T}{N}\sum_{q,l} e^{iq(f-f')-i\omega_l(\tau-\tau')} D_{++}(q, i\omega_l) \\ (\omega_l = 2l\pi T, \quad l = 0, \pm1, \pm2, \ldots),\end{aligned} \tag{17}$$

the expression

$$D_{++}(q, i\omega_l) = G_{++}(q, i\omega_l) P(q, i\omega_l) \tag{18}$$

was obtained, where

$$G_{++}(q,i\omega_l) = \frac{i\omega_l}{(i\omega_l)^2 - \tilde{\Omega}_q^2(i\omega_l)},$$

$$P(q,i\omega_l) = \frac{2}{3i\omega_l}\frac{1}{N}\sum_p C_p(I_{q-p} - I_p), \quad (19)$$

$$\tilde{\Omega}_q^2(i\omega_l) = \frac{1}{3N}\sum_q C_q\left(I_q - I_k - \Pi_k(i\omega_l)\right)(I_q - I_{k-q}).$$

Here,

$$I_q = I\sum_\delta e^{-iq\delta} = 4I\gamma_{1q} \quad \text{and} \quad C_q = \sum_\delta e^{-iq\delta}C_\delta, \quad (20)$$

where $\gamma_{1q} = (\cos k_x + \cos k_y)/2$ is the lattice invariant, are the Fourier transforms of the exchange integral I_{fm} and correlation function C_{fm}, respectively, and $\Pi_k(i\omega_l)$ is the polarization operator including the effect of charge carriers on the spin subsystem.

The expression for the spin Green's function can be written in a simpler form taking into account that the exchange interaction only between the nearest neighbor spins is included and using the static approximation for the polarization operator $\Pi_k(i\omega_l) = \Pi_k$:

$$D_{++}(q,i\omega_l) = \frac{(8/3)C_1 I(\gamma_{1q} - 1)}{(i\omega_l)^2 - \Omega_q^2}. \quad (21)$$

Here, Ω_q is the dispersion relation for spin-wave excitations:

$$\Omega_q^2 = \frac{16}{3}I^2|C_1|(1-\gamma_{1q})\left[1 + \gamma_{1q} + \Delta_q\right], \quad (22)$$

where

$$\Delta_q = \frac{3/4 + 2C_2 + C_3}{4|C_1|} - 1 + \frac{\Pi_q}{4I} \quad (23)$$

is the function describing the gap in the spectrum of spin excitations near the (π, π) point of the Brillouin zone and C_j is the spin correlator of the jth coordination sphere, which should be determined self-consistently in terms of the spin Green's function as

$$C_j = \frac{3}{2}\frac{T}{N}\sum_{q,l} e^{iq\delta_j} D_{++}(q,i\omega_l), \quad (24)$$

where δ_j is the vector connecting sites from the jth coordination sphere.

To calculate the doping dependence of the spin correlation function, we replace the polarization operator Π_q in the spectrum Ω_q by its average value over the Brillouin zone Π. Further, we take into account that the gap $\Delta_Q(\Pi)$ given by Eq. (23) at $q = Q \equiv (\pi, \pi)$ is linearly related to the inverse magnetic correlation length ξ^{-1}. According to the experimental data on neutron scattering and nuclear magnetic resonance (see, e.g., [41, 42]), the inverse magnetic correlation length ξ^{-1} depends on the doping x and this parameter for lanthanum superconductors increases by several times with increasing x in the range of 0.03–0.3. According to these data, the value of the averaged polarization operator Π for each doping x is chosen such that the spin gap increases by a factor of 2.5 with increasing x from 0.03 to 0.3.

5. SINGLE-LOOP APPROXIMATION FOR THE SELF-ENERGY PART

The first-order contributions in the exchange interaction J to the mass operator given by Eq. (13) vanish because the spin system is in the quantum spin liquid phase. The first nonzero contributions appear in the second order and are described by one-loop diagrams shown in Fig. 1. According to the general rules [13, 31], the solid line with arrow in these diagrams corresponds to the Green's function of noninteracting holes $G_k^{(0)}(i\omega_m)$. Each wavy line corresponds to the interaction strength J; the wavy line with the empty circle corresponds to the longitudinal spin–fermion interaction and the wavy line without circle corresponds to the transverse interaction. The double dashed line with the black semicircle means the spin Green's function $D_{++}(q,i\omega_l) = G_{++}(q,i\omega_l)P(q,i\omega_l)$, where the dashed line corresponds to the propagator $G_{++}(q,i\omega_l)$ and the semicircle stands for the terminal factor $P(q,i\omega_l)$. The shaded oval in Fig. 1b corresponds to the Fourier transform of Green's function

$$D_{zz}(f\tau; f'\tau') = -\langle T_\tau S_f^z(\tau)S_{f'}^z(\tau')\rangle. \quad (25)$$

Two ν_q factors corresponding to the input, $G_q^{(0)}(i\omega_m)$, and output fermion Green's functions are attributed to each vertex. The law of energy and momentum conservation is satisfied at all the vertices.

Since

$$D_{zz}(q,i\omega_l) = \frac{1}{2}D_{++}(q,i\omega_l) \quad (26)$$

according to the SU(2) invariance of the ground state of the spin subsystem, the one-loop diagrams shown

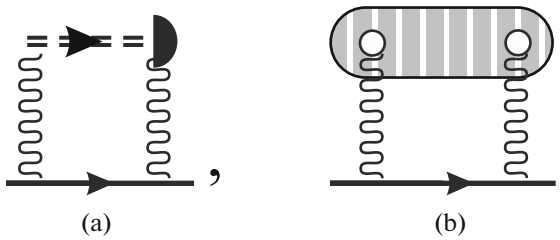

Fig. 1. One-loop diagrams for the mass operator.

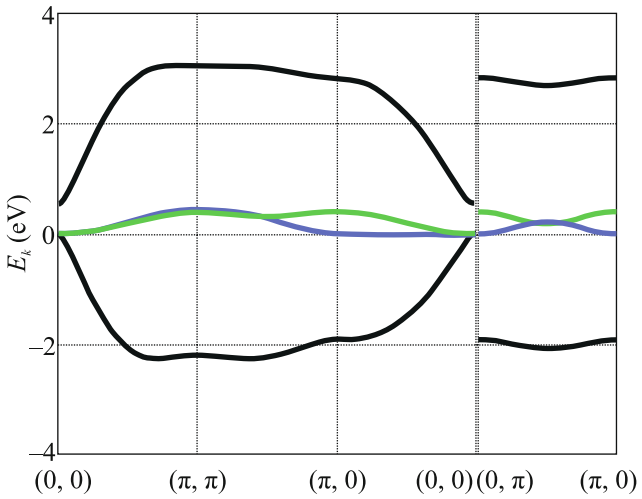

Fig. 2. (Black lines) Energy spectrum of spin polarons calculated in the one-loop approximation and (blue and green lines) the spectrum of holes of the oxygen subsystem.

in Figs. 1a and 1b can be represented in the form of the analytical expressions

$$\Sigma^{(a)}(k, i\omega_m) = -J_{kk}\bar{Y}_k(i\omega_m), \quad (27)$$

$$\Sigma^{(b)}(k, i\omega_m) = -\frac{1}{2}J_{kk}\bar{Y}_k(i\omega_m), \quad (28)$$

where

$$\bar{Y}_k(i\omega_m) = \frac{T}{N}\sum_{p,n} J_{k-p,k-p}G^{(0)}_{k-p}(i\omega_{m-n})D_{++}(p, i\omega_n).$$

The energy spectrum of spin-polaron quasiparticles is determined by the poles of the retarded Green's function obtained by the analytic continuation of the Matsubara Green's function given by Eq. (11), which is performed in this case on the basis of Padé approximants [43]. The spectrum calculated in the one-loop approximation for the self-energy part specified by Eq. (13) is shown by black lines in Fig. 2 in comparison with the bare spectrum of "bare" holes of the subsystem of oxygen ions shown by the blue and green lines.

We emphasize two important features of the spin-polaron spectrum in Fig. 2, which were noted previously in [18, 19], where the energy structure of spin-polaron quasiparticles was analyzed within the spin–fermion model using the Zwanzig–Mori projection technique [25, 26]. The first feature is a significant decrease (by almost 2 eV) in the energy of spin-polaron states owing to the strong coupling of oxygen holes with the spin subsystem. For low doping levels characteristic of cuprate superconductors, states corresponding to the bottom of the lower band in Fig. 2 are filled. The second feature of the presented spectrum is the formation of a local minimum near the $(\pi/2, \pi/2)$ point of the Brillouin zone. This feature leads to the characteristic shape of the Fermi surface in weakly doped cuprates in the form of a hole pocket.

6. LADDER DIAGRAM APPROXIMATION FOR THE SELF-ENERGY PART

A disadvantage of the spin-polaron spectrum in Fig. 2 is the absence of the third important feature—the splitting of the lower spin-polaron band from the band of bare hole states by a gap of about 1–2 eV—mentioned in [18, 19].

Using the bundle diagram technique, we recently showed [29] that the processes of multiple scattering of holes on the same localized copper spin subsystem is responsible for the appearance of the gap between the lower spin-polaron band and the upper bare band. Within our approach based on the diagram technique for spin operators, such processes are involved, in particular, in the infinite series of ladder diagrams shown in Fig. 3. This series begins with the diagram shown in Fig. 1a, which is supplemented by diagrams appearing from this diagram by adding longitudinal interaction lines. In view of the split character of the spin–fermion interaction function J_{kq} mentioned in Section 2, it is easy to sum the analytical contributions from the terms of the series shown in Fig. 3 and to obtain the following expression for the corresponding self-energy part:

$$\Sigma^{(A)}(k, i\omega_m) = \frac{-J_{kk}\bar{Y}_k(i\omega_m)}{1 - Y_k(i\omega_m)}, \quad (29)$$

where

$$Y_k(i\omega_m) = \frac{T}{N}\sum_{p,n} J_{k-p,k-p}G^{(0)}_{k-p}(i\omega_{m-n})G_{++}(p, i\omega_n).$$

The energy spectrum of spin polarons calculated in the ladder approximation, where the mass operator is approximated by the sum of the self-energy parts $\Sigma^{(A)}$

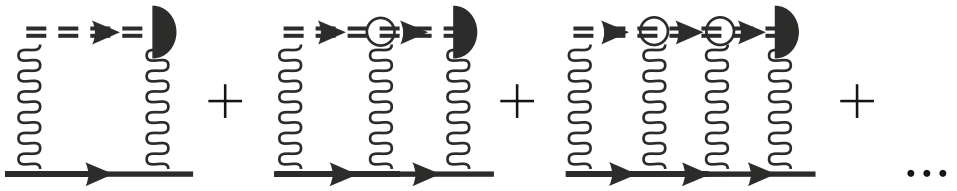

Fig. 3. Series of ladder diagrams representing the processes of multiple scattering of holes on localized spins.

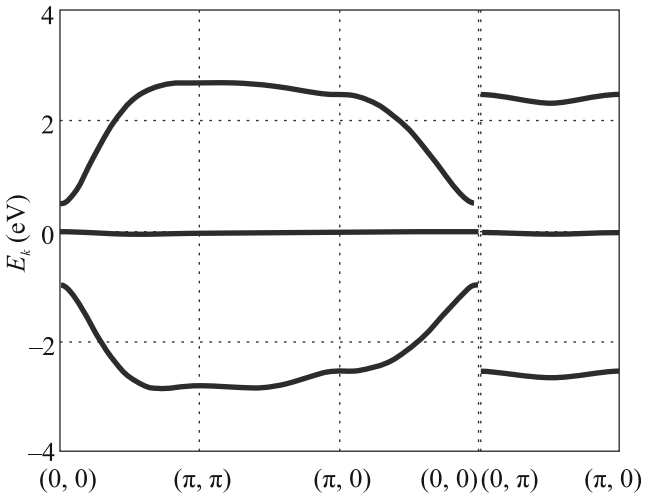

Fig. 4. Energy spectrum of spin polarons calculated in the ladder approximation.

(29) and $\Sigma^{(b)}$ (28), is shown in Fig. 4. The comparison of the spectrum in Fig. 2, which is obtained in the one-loop approximation, with the spectrum in Fig. 4 indicates a qualitative difference that is the splitting of the band of spin-polaron quasiparticles from the band of "bare" holes by 1 eV. Furthermore, the third band with weak dispersion, which is absent in Fig. 2, appears near zero in Fig. 4.

7. CONCLUSIONS

To summarize, the concept of the spin polaron in cuprate superconductors has been implemented for the first time within the diagram technique for fermion and spin operators. Considering the hole and spin subsystems on the CuO_2 plane within the spin–fermion model, we have chosen the minimum set of one-loop and ladder diagrams for the self-energy part of the fermion Green's function that are necessary to reproduce the most important features of the spectrum of spin-polaron quasiparticles. It has been shown that, for a significant decrease in the energy of spin-polaron quasiparticles and the formation of a local minimum of the energy spectrum near the $(\pi/2, \pi/2)$ point of the Brillouin zone, it is sufficient to take into account only one-loop diagrams. However, to obtain an energy gap between the lower branch of spin-polaron states and the upper branches of oxygen holes, it is necessary to take into account the ladder diagrams for the self-energy part of the fermion Green's function. These diagrams ensure good qualitative agreement of the spin-polaron spectrum obtained using the diagram approach with the results of previous works, where the energy structure of spin-polaron quasiparticles was studied using the Zwanzig–Mori projection technique. We believe that the approach developed in this work will be an efficient tool for the description of the pseudogap phase of cuprate superconductors, where spin-polaron quasiparticles serve as charge carriers.

FUNDING

This work was supported by the Russian Foundation for Basic Research, project nos. 18-02-00837 and 20-32-70059.

REFERENCES

1. A. F. Barabanov, R. O. Kuzian, and L. A. Maksimov, Phys. Rev. B **55**, 4015 (1997).
2. A. F. Barabanov, O. V. Urazaev, A. A. Kovalev, and L. A. Maksimov, JETP Lett. **68**, 412 (1998).
3. A. F. Barabanov, A. V. Mikheenkov, and A. M. Belemuk, JETP Lett. **75**, 107 (2002).
4. V. V. Val'kov, D. M. Dzebisashvili, M. M. Korovushkin, and A. F. Barabanov, Phys. Usp. **64** (2021, in press).
5. M. Vojta, Adv. Phys. **58**, 699 (2009).
6. B. Keimer, S. A. Kivelson, M. R. Norman, S. Uchida, and J. Zaanen, Nature (London, U.K.) **518**, 179 (2015).
7. N. Plakida, *High-Temperature Cuprate Superconductors: Experiment, Theory, and Applications* (Springer, Dordrecht, 2010).
8. N. M. Plakida, L. Anton, S. Adam, and G. Adam, J. Exp. Theor. Phys. **97**, 331 (2003).
9. A. A. Vladimirov, D. Ile, and N. M. Plakida, Theor. Math. Phys. **152**, 1331 (2007).
10. Yu. A. Izyumov, Phys. Usp. **38**, 385 (1995).
11. Yu. A. Izyumov, Phys. Usp. **40**, 445 (1997).
12. M. V. Eremin, S. G. Solov'yanov, and S. V. Varlamov, J. Exp. Theor. Phys. **85**, 963 (1997).
13. S. G. Ovchinnikov and V. V. Val'kov, *Hubbard Operators in the Theory of Strongly Correlated Electrons* (Imperial College Press, London, 2004).
14. L. A. Maksimov, R. Hayn, and A. F. Barabanov, Phys. Lett. A **238**, 288 (1998).
15. Yu. A. Izyumov and Yu. N. Skryabin, *Basic Models in Quantum Theory of Magnetism* (UrO RAN, Ekaterinburg, 2002) [in Russian].
16. V. V. Val'kov, M. M. Korovushkin, and A. F. Barabanov, JETP Lett. **88**, 370 (2008).
17. A. F. Barabanov, L. A. Maksimov, and G. V. Uimin, JETP Lett. **47**, 622 (1988).
18. A. F. Barabanov, A. A. Kovalev, O. V. Urazaev, A. M. Belemuk, and R. Hayn, J. Exp. Theor. Phys. **92**, 677 (2001).
19. D. M. Dzebisashvili, V. V. Val'kov, and A. F. Barabanov, JETP Lett. **98**, 528 (2013).
20. V. V. Val'kov, D. M. Dzebisashvili, and A. F. Barabanov, Phys. Lett. A **379**, 421 (2015).
21. V. V. Val'kov, D. M. Dzebisashvili, M. M. Korovushkin, and A. F. Barabanov, JETP Lett. **103**, 385 (2016).
22. V. V. Val'kov, D. M. Dzebisashvili, M. M. Korovushkin, and A. F. Barabanov, J. Low Temp. Phys. **191**, 408 (2018).

23. V. J. Emery, Phys. Rev. Lett. **58**, 2794 (1987).
24. C. M. Varma, S. Schmitt-Rink, and E. Abrahams, Solid State Commun. **62**, 681 (1987).
25. R. Zwanzig, Phys. Rev. **124**, 983 (1961).
26. H. Mori, Prog. Theor. Phys. **33**, 423 (1965).
27. Yu. A. Tserkovnikov, Sov. J. Theor. Math. Phys. **49**, 993 (1981).
28. D. M. Dzebisashvili and K. K. Komarov, Eur. Phys. J. B **91**, 278 (2018).
29. V. V. Val'kov, V. A. Mitskan, M. M. Korovushkin, D. M. Dzebisashvili, and A. F. Barabanov, J. Low Temp. Phys. **197**, 34 (2019).
30. A. A. Abrikosov, L. P. Gor'kov, and I. E. Dzyaloshinskii, *Methods of Quantum Field Theory in Statistical Physics* (Fizmatgiz, Moscow, 1962; Prentice-Hall, Englewood Cliffs, NJ, 1963).
31. Yu. A. Izyumov, F. A. Kossan-Ogly, and Yu. N. Skryabin, *Field Methods in the Theory of Ferromagnetism* (Nauka, Moscow, 1974) [in Russian].
32. R. O. Zaitsev and V. A. Ivanov, Sov. Phys. Solid State **29**, 1475 (1987).
33. P. Prelovšek, Phys. Lett. A **126**, 287 (1988).
34. J. Zaanen and A. M. Oleś, Phys. Rev. B **37**, 9423 (1988).
35. E. B. Stechel and D. R. Jennison, Phys. Rev. B **38**, 4632 (1988).
36. V. J. Emery and G. Reiter, Phys. Rev. B **38**, 4547 (1988).
37. H. Matsukawa and H. Fukuyama, J. Phys. Soc. Jpn. **58**, 2845 (1989).
38. B. S. Shastry, Phys. Rev. Lett. **63**, 1288 (1989).
39. D. F. Digor and V. A. Moskalenko, Theor. Math. Phys. **130**, 271 (2002).
40. V. V. Val'kov, D. M. Dzebisashvili, and A. F. Barabanov, Theor. Math. Phys. **191**, 752 (2017).
41. B. Keimer, N. Belk, R. J. Birgeneau, A. Cassanho, C. Y. Chen, M. Greven, M. A. Kastner, A. Aharony, Y. Endoh, R. W. Erwin, and G. Shirane, Phys. Rev. B **46**, 14034 (1992).
42. V. Barzykin and D. Pines, Phys. Rev. B **52**, 13585 (1995).
43. H. J. Vidberg and J. W. Serene, J. Low Tem. Phys. **29**, 179 (1977).

Translated by R. Tyapaev